View metadata, citation and similar papers at core.ac.uk
brought to you by CORE
provided by Repository@USM

HEAT TRANSFER AND DEFORMATION OF FLEXIBLE PRINTED CIRCUIT BOARD WITH MULTI BALL GRID ARRAY PACKAGES

LIM CHONG HOOI

UNIVERSITI SAINS MALAYSIA
2017

HEAT TRANSFER AND DEFORMATION OF FLEXIBLE PRINTED CIRCUIT BOARD WITH MULTI BALL GRID ARRAY PACKAGES

by

LIM CHONG HOOI

Thesis submitted in fulfilment of the requirements for the degree of Doctor of Philosophy

June 2017

ACKNOWLEDGEMENTS

First and foremost, I would like to express my sincerest gratitude to my supervisor, Prof. Ir. Dr. Mohd. Zulkifly Abdullah for his constant encouragement, valuable suggestions and guidance in making this research project successful. As a mentor, he has provided me with consistent support on the project with his knowledge and patience, while allowing me the room to work and learn on my own. Besides, I also wish to express my sincere thanks to my co-supervisor, Prof. Dr. Ishak Haji Abdul Azid for his obliged discussions and opinions on the research.

Furthermore, I would like to thank Dean, Prof. Dr. Zainal Alimuddin Zainal Alauddin, Mr. Fakruruzi, Mr. Jamari, Mr. Sani, Mr. Latif, Mr. Rosni, Mr. Amri and all involved staffs of the School of Mechanical Engineering, Universiti Sains Malaysia for their countless assistances and supports. Besides, I would also like to thank Prof. Ahmad Shukri Yahya, Dr. Khor Chu Yee, Dr. Mohd Sharizal Abdul Aziz for clearing the doubt in RSM optimization and sharing their knowledge on numerical simulation.

A special thank goes to the Malaysian Ministry of Higher Education for the funding through the MyBrain15 programme. Last but not least, I would like to thank my loving parents and friends for their continuous support and encouragements throughout my Ph.D. studies at USM. For those who have directly and indirectly contributed to the accomplishment of this research, thank you very much.

TABLE OF CONTENTS

	Page
ACKNOWLEDGEMENTS	ii
TABLE OF CONTENTS	iii
LIST OF TABLES	vii
LIST OF FIGURES	viii
LIST OF ABBREVIATIONS	xii
LIST OF SYMBOLS	xiii
ABSTRAK	xvi
ABSTRACT	xviii
CHAPTER ONE: INTRODUCTION	
1.1 Introduction	1
1.2 Printed Circuit Board	2
1.2.1 Rigid PCB	2
1.2.2 Flexible PCB	3
1.3 Problem Statements	4
1.4 Research Objectives	5
1.5 Scope of Research Work	5
1.6 Thesis Outline	7
CHAPTER TWO: LITERATURE REVIEW	
2.1 Introduction	8
2.2 Rigid Printed Circuit Board	8

2.2.1 Thermal Stress on RPCB 8
2.2.2 Flow on RPCB 11
2.2.3 Mechanical Study for RPCB 15
2.2.4 Empirical Correlation 17
2.3 Flexible Printed Circuit Board 19
2.3.1 Thermal Effect on FPCB 19
2.3.2 Mechanical Study for FPCB 21
2.3.3 Application of FPCB 22
2.4 Fluid-Structure Interaction 24
2.5 Optimizing Parameters for Better Performance 27
2.6 Findings/Remarks on Literature Review 28

CHAPTER THREE: METHODOLOGY

3.1 Introduction 32
3.2 FPCB Thermal and Material Testing 34
3.3 Theoretical Background 35
3.4 Numerical Simulation 37
3.5 FSI Fluid Modelling – FLUENT 39
3.5.1 Modelling and Mesh Development 39
3.5.2 Simulation Setup 40
3.6 FSI Structural Modelling – ABAQUS 42
3.6.1 Modelling 42
3.6.2 BGA Assembly Mechanical Properties 43
3.6.3 Simulation Setup and Mesh Development 44
3.7 MpCCI Coupling for FSI Setup 45
3.8 Thermal and FSI Coupling 47
3.8.1 FLUENT 47

3.8.2 ABAQUS 48

3.8.3 MpCCI Coupling for Thermal and Flow Properties Setup 49

3.9 Grid Independency Test 49

3.10 Experiment 51

3.10.1 Test Vehicle 51

3.10.2 Experimental Setup 52

3.11 Parametric Model Development 55

3.12 RSM Optimization 59

3.13 Empirical Correlation 62

3.14 Summary 63

CHAPTER FOUR: RESULTS AND DISCUSSION

4.1 Introduction 64

4.2 Validation of Developed Numerical Simulation 65

4.3 Thermal and Material Properties of FPCB 66

4.4 BGA Assembly without Heat Source 67

4.4.1 Experimental Results 67

4.4.2 Comparison of Experiment Results with Numerical Predictions 68

4.4.3 Effect of *Re* 69

4.4.4 Effect of Component Quantity 71

4.5 BGA Assembly with Heat Source at BGA Packages' surface 72

4.5.1 Experimental Results 72

4.5.2 Comparison of Experiment Results with Numerical Predictions 73

4.6 Comparison for Cases without and with Heat Source 75

4.7 Comparison of FPCB and RPCB 77

4.8 BGA Assembly with Heat Source in Actual Operating Condition 79

4.8.1 Effect of Re 80

4.8.2 Effect of Number of BGA Packages 82

4.8.3 Effect of Thermal Power 83

4.8.4 Effect of FPCB's Size 85

4.8.5 Effect of Distance between BGA 87

4.8.6 RSM Optimization 89

4.8.7 Empirical Correlation 113

CHAPTER FIVE: CONCLUSION AND RECOMMENDATIONS

5.1 Conclusion 116

5.1.1 Heat Transfer Enhancement of FPCB 116

5.1.2 Factors Investigation and Empirical Correlation 117

5.1.3 RSM Optimization 118

5.2 Recommendations 119

REFERENCES 120

APPENDICES

LIST OF PUBLICATIONS

LIST OF TABLES

		Page
Table 2.1	Constants of Equation (2.6) for Tso et al. (1999) study.	18
Table 3.1	Mechanical properties used in the BGA assembly.	44
Table 3.2	Thermal properties used in the BGA assembly.	48
Table 3.3	Grid independency test for fluid domain.	50
Table 3.4	Grid independency test for structural domain.	50
Table 3.5	Dimensions of the BGA assembly.	51
Table 3.6	Cases description.	57
Table 3.7	Variations of factors.	58
Table 3.8	Levels of factors for 1 – 3 number of BGA packages.	60
Table 3.9	Levels of factors for 4 number of BGA packages.	61
Table 4.1	Comparison of thermal coupling simulation method with Grimes's experiment.	66
Table 4.2	Measured material and thermal properties of FPCB.	66
Table 4.3	Comparison with RPCB.	78
Table 4.4	Results of the central composite design for 1 – 3 BGA packages.	91
Table 4.5	Results of the central composite design for 4 BGA packages.	92
Table 4.6	ANOVA of the 2FI and quadratic models.	94
Table 4.7	Optimized Re for each number of BGA packages attached.	113
Table 4.8	Values for Equation (4.8) unknown.	114
Table 4.9	Comparison of $\overline{Nu}$ obtained from simulation and correlation equations.	115

LIST OF FIGURES

		Page
Figure 1.1	Rigid PCB in mobile phone (Ji et al., 2010).	2
Figure 1.2	Typical flexible PCB (Rizvi et al., 2010).	4
Figure 2.1	Flanged Tubelet installation (Berkebile, 1967).	9
Figure 2.2	Material property distribution inside PCB (Yaddanapudi et al., 2015).	11
Figure 2.3	RPCB with paint exposed to air flow for 15 seconds (Eveloy et al., 2000).	13
Figure 2.4	Grimes experimental setup (Grimes and Davies, 2002).	14
Figure 2.5	Multi-component PCB model by (Rodgers et al., 2003a).	15
Figure 2.6	Depaneling case study (Lau et al., 2006).	17
Figure 2.7	One-quarter chip resistor solder joint on FPCB modelling (Rizvi et al., 2010).	20
Figure 2.8	Peel test for RPCB-FPCB electrode bonding (Yoon et al., 2013).	22
Figure 2.9	FPCB antenna design (Kuo-Liang et al., 2010).	23
Figure 2.10	Postal security on envelope (Siegel et al., 2010).	23
Figure 2.11	Various factors in FPCB analysis (Leong et al., 2013a).	26
Figure 2.12	Test vehicle for Leong and Abdullah (2012) experimental setup.	27
Figure 2.13	Amount of literatures reviewed for PCB.	29
Figure 3.1	Research flow chart.	33
Figure 3.2	Hot Disk Thermal Analyser (a) TPS 2500 S (b) sensor with setup.	34
Figure 3.3	Distributed force on two ends of fixed structural.	35
Figure 3.4	MpCCI Coupling Process.	38

Figure 3.5	Fluid domain.	39
Figure 3.6	Meshed fluid domain.	40
Figure 3.7	Flow chart of fluid domain modelling.	42
Figure 3.8	Structural domain.	43
Figure 3.9	Flow chart of structural domain modelling.	45
Figure 3.10	Structural domain mesh and boundary conditions.	45
Figure 3.11	Overview of MpCCI setup.	47
Figure 3.12	Cross section view of BGA assembly.	51
Figure 3.13	Desktop lead-free reflow oven TYR108C.	52
Figure 3.14	Test vehicle.	52
Figure 3.15	Schematic diagram of the experimental setup.	54
Figure 3.16	Experimental setup.	54
Figure 3.17	Preliminary study model.	55
Figure 3.18	1 – 4 number of BGA packages models.	56
Figure 3.19	Measured temperature locations.	57
Figure 4.1	Comparison of FSI simulation method with previous work.	65
Figure 4.2	Stress-strain curve of FPCB.	67
Figure 4.3	Experiment measurements at maximum δ point for Case 1.1 and Case 2.1.	68
Figure 4.4	Comparison between experiment and numerical results for (a) Case 1.1 and (b) Case 2.1.	69
Figure 4.5	δ and von Mises stress contour on Case 1.1 from Re = 7680 - 38400.	70
Figure 4.6	δ/L vs Re for different numbers of BGA packages.	71
Figure 4.7	von Mises stress vs Re for different number of BGA packages.	71

Figure 4.8	Experiment measurements at maximum δ point for Case 1.2 and Case 2.2.	73
Figure 4.9	Experiment measurements at maximum temperature location for Case 1.2 and Case 2.2.	73
Figure 4.10	Comparison between experiment and numerical results for (a) δ and (b) temperature.	74
Figure 4.11	Comparison of δ/L between cases with and without heat source in simulation.	76
Figure 4.12	Comparison of von Mises stress between cases with and without heat source in simulation.	77
Figure 4.13	Contour of maximum von Mises stress on Case 2.2 at *Re* = 7680 with cross section enlargement.	77
Figure 4.14	$\overline{Nu}$ of FPCB and RPCB with 1 BGA package attached.	79
Figure 4.15	Pressure different from ambient pressure for FPCB and RPCB.	79
Figure 4.16	Comparison of δ/L vs *Re* from 1- 4 BGA packages.	81
Figure 4.17	Comparison of von Mises stress vs *Re* from 1- 4 BGA packages.	81
Figure 4.18	Comparison of $\overline{Nu}$ vs *Re* from 1- 4 BGA packages.	81
Figure 4.19	Comparison of δ/L vs *Re* from 0 - 0.213 W.	84
Figure 4.20	Comparison of von Mises stress vs *Re* from 0 - 0.213 W.	84
Figure 4.21	Comparison of $\overline{Nu}$ vs Re from 0 - 0.213 W.	85
Figure 4.22	Comparison of δ on different sizes with various velocities.	86
Figure 4.23	Comparison of von Mises stress on different sizes with various velocities.	87
Figure 4.24	Comparison of $\bar{h}$ on different sizes with various velocities.	87
Figure 4.25	δ vary with the distance between BGA packages	88

Figure 4.26 von Mises stress vary with the distance between BGA packages 89

Figure 4.27 *h* vary with the distance between BGA packages 89

Figure 4.28 Perturbation plot for (a) 1 - 3 BGA packages maximum δ/L ($Y_{1.1}$) (b) 4 BGA packages maximum δ/L ($Y_{2.1}$). 98

Figure 4.29 Perturbation plot for (a) 1 - 3 BGA packages von Mises stress ($Y_{1.2}$) (b) 4 BGA packages von Mises stress ($Y_{2.2}$). 99

Figure 4.30 Perturbation plot for (a) 1 - 3 BGA packages $\overline{Nu}$ ($Y_{1.3}$) (b) 4 BGA packages $\overline{Nu}$ ($Y_{2.3}$). 100

Figure 4.31 Interaction plots and 3D response surface of maximum δ/L ($Y_{1.1}$) for (a) *AB* (b) *AC* (c) *BC*. 102

Figure 4.32 Interaction plots and 3D response surface of von Mises stress ($Y_{1.2}$) for (a) *AB* (b) *AC* (c) *BC*. 106

Figure 4.33 Interaction plots and 3D response surface of $\overline{Nu}$ ($Y_{1.3}$) for (a) *AB* (b) *AC* (c) *BC*. 109

Figure 4.34 Simulation and empirical equations results. 115

LIST OF ABBREVIATIONS

2D	Two dimensional
2FI	Two factor-interactions
3D	Three dimensional
ADPI	Air diffusion performance index
ANOVA	Analysis of variance
ATC	Accelerated thermal cycling
BGA	Ball grid array
CAD	Computer-aided design
CCD	Central composite design
CFD	Computational fluid dynamic
CTE	Coefficient of thermal expansion
FEM	Finite element method
FPCB	Flexible printed circuit board
FSI	Fluid-structure interaction
IC	Integrated circuit
LED	Light-emitting diode
MpCCI	Multi-physics Code Coupling Interface
PCB	Printed circuit board
RFID	Radio-frequency identification
RPCB	Rigid printed circuit board
RSM	Response surface method
TPS	Transient plane source

LIST OF SYMBOLS

δ	Deflection
ρ_f	Fluid density
ρ_s	Structure density
μ_f	Fluid dynamic viscosity
μ_m	Dynamic viscosity at channel entrance
μ_s	Structure dynamic viscosity
μ_w	Dynamic viscosity at wall of heat source
σ_x	Standard deviation
$\sigma_{\bar{x}}$	Standard error
σ_y	Yield strength
$\vec{\sigma}$	Recoverable stress
α	Thermal expansion coefficient
β_0	Constant coefficient
β_i	Linear coefficient
β_{ii}	Quadratic coefficient
β_{ij}	Second order interaction coefficient
A	RSM code for *Re*
a	Surface area
B	RSM code for thermal power
b	Component’s height
C	RSM code for number of BGA packages
c	Constant

C_p	Specific heat
E	Young's modulus
e	Random error
g	Gravity
H	Wind tunnel's height
h	Heat transfer coefficient
$\overline{h}$	Average heat transfer coefficient
k_f	Fluid thermal conductivity
k_s	Structure thermal conductivity
L	Characteristic length
l	Component's width
N	Sample size
Nu	Local Nusselt number
$\overline{Nu}$	Average Nusselt number
n	Total number of factors
P	Pressure
Pr	Prandtl number
q	Convection heat transfer energy
R^2	Coefficient of determination
Re	Reynolds number
Re^m	Reynolds number at the channel entrance
T	Temperature
T_s	Surface temperature
T_∞	Freestream temperature

t	Time
t_d	t-distribution value on the level of confidence
U	Linear displacement
UR	Rotational displacement
u_f, v_f, w_f	Fluid flow velocity in x, y and z axis correspondingly
$\overrightarrow{u_s}$	Structure overall velocity vector
X	Independent variable
x_o	Unheated starting length
$\bar{x}$	Mean value
Y	Response variable

PEMINDAHAN HABA DAN DEFORMASI FLEKSIBEL PAPAN LITAR TERCETAK DENGAN PELBAGAI BILANGAN PAKEJ JARINGAN GRID BOLA

ABSTRAK

Teknologi elektronik dan mikroelektronik yang berkembang pantas meningkatkan permintaan terhadap peranti elektronik yang fleksibel dan ringan. Papan Litar Tercetak Fleksibel (FPCB) yang digunakan untuk menggantikan Papan Litar Tercetak Tegar (RPCB) dilengkapi dengan ciri-ciri tersebut. Walaubagaimanapun, ciri-ciri lembut yang terdapat pada FPCB menghadapi pesongan (δ) yang tidak diperlukan dan tegasan yang hadir daripada aliran dan haba yang dijana daripada komponen-komponen semasa operasi. Di dalam penyelidikan yang dijalankan, kesan haba dan aliran terhadap FPCB dengan pakej Jaringan Grid Bola (BGA) telah berganding secara setemu di dalam simulasi untuk mengkaji kesannya terhadap FPCB. Kesan-kesan aliran telah dikaji pada permulaan penyelidikan, diikuti dengan penambahan sumber haba terhadap pakej BGA. Disamping itu, pemindahan haba yang 24 % lebih tinggi pada FPCB telah ditunjukkan apabila dibandingkan dengan RPCB. Beberapa faktor parametrik telah dikaji termasuklah halaju aliran (v) (1 – 5 m/s), 1 - 4 pakej BGA yang dilampirkan, sumber kuasa (0 – 0.213 W) yang dikenakan pada pakej BGA, saiz FPCB (80mm^2 – 140mm^2) dan jarak antara pakej BGA (15 mm – 45 mm). Disamping itu, kecekapan pemindahan haba (h) telah ditambah sebagai tindak balas terhadap kajian pemindahan dalam kes yang melibatkan sumber haba. Kemudian v, δ dan h telah dinormalkan kepada nombor Reynolds (Re), δ/panjang FPCB (L) dan nombor Nusselt ($\overline{Nu}$) yang tidak berdimensi. Kebanyakan faktor-faktor parametrik telah dijumpai amat mempengaruhi tegasan δ/L dan $\overline{Nu}$. Tambahan pula, pengoptimuman

telah dijalankan melalui kaedah permukaan tindakbalas (RSM) bagi menyediakan pendekatan rekabentuk yang berasaskan faktor-faktor dalam kajian awal untuk kepentingan jurutera dan perekabentuk FPCB. Berdasarkan penemuan penyelidikan, pengaruh aliran lebih tinggi terhadap tindak balas apabila sumber haba rendah. Sebaliknya, pengaruh haba lebih tinggi daripada pengaruh aliran apabila sumber haba tinggi. Selain itu, korelasi empirik $\overline{Nu}$, *Re*, nombor Prandtl (*Pr*) dan δ/L telah berjaya ditemukan, di mana pengaruh yang paling tinggi ialah *Re* diikuti oleh *Pr* dan δ/L. Di dalam penyelidikan terkini, di bawah pengaruh aliran dan sumber haba, δ/L, tegasan dan $\overline{Nu}$ yang tertinggi boleh mencecah 0.0043, 8.69 MPa and 85.54. Oleh itu, adalah amat penting untuk mengambilkira aspek haba bersama pengaruh aliran untuk mendapatkan ciri-ciri FPCB bersama pakej BGA semasa operasi. Kejayaan simulasi ini boleh membantu kajian tentang ciri-ciri fleksibel substrat dengan komponen yang beroperasi di bawah pengaruh aliran.

HEAT TRANSFER AND DEFORMATION OF FLEXIBLE PRINTED CIRCUIT BOARD WITH MULTI BALL GRID ARRAY PACKAGES

ABSTRACT

The rapid development of electronic and microelectronic technology increases the demands for electronics device with flexible and light weight capability. Flexible printed circuit board (FPCB) which can be used to replace rigid printed circuit board (RPCB) is well equipped with those features. However, the soft feature of FPCB poses unwanted deflection (δ) and stress from the flow and heat generated by the operating components. In present research, thermal and flow effects on FPCB with attached ball grid array (BGA) packages have been investigated where the numerical simulation with coupled of flow and thermal effects concurrently has been successfully developed in the simulation. The effects of flow are studied at the initial stage of the research, followed by the addition of heat source to the BGA packages. The experimental work with actual attached ball grid array (BGA) packages was carried out to verify and validate the results. Findings show that better heat transfer performance on FPCB with an average 24 % higher than RPCB. Several parametric factors are explored including flow velocities (v) (1 – 5 m/s), 1 - 4 number of BGA packages attached, power supplied to the BGA packages (0 – 0.213 W), size of FPCB (80mm^2 – 140mm^2) and distance between BGA packages (15 mm – 45 mm). The heat transfer coefficient (h) has been added into the responses to study the heat transfer in the cases that involved heat source. Later on, v, δ and h had been normalized into dimensionless Reynolds number (Re), δ/length of FPCB (L) and Nusselt number ($\overline{Nu}$), respectively. Most the parametric factors were found to be significantly affected the δ/L, stress and $\overline{Nu}$. Optimization is then carried out by response surface methodology (RSM) to provide the design approaches based on

those factors in present study for the interests of FPCB designers or engineers. Based on the results and findings, the flow has significant effect on the responses when thermal power is low. On the other hand, the thermal effect is higher than flow when thermal power is high. Besides, empirical correlation equations of Re, Prandtl number (Pr), δ/L and $\overline{Nu}$ has been established, in which the highest effect is Re, followed by Pr and δ/L. In present research, under the influences of flow and thermal power supplied, the highest δ/L, stress and $\overline{Nu}$ could reach 0.0043, 8.69 MPa and 85.54, respectively. Therefore, it is important to consider thermal effect together with flow influences for understanding the characteristic of FPCB attached with BGA under operating condition. With the successful development of thermal-mechanical-fluid-structure interaction numerical coupling method, in which thermal and flow effects have been considered simultaneously could help to study flexible substrate characteristic under operating condition and flow environment which is closer to real life scenario.

CHAPTER ONE

INTRODUCTION

1.1 Introduction

The high demand of electronic devices has caused the rapid growth of electronic and microelectronic industries since the past few decades. The devices such as smart phone, laptop, computer, tablet etc. have penetrated into the daily life and greatly improve the lifestyle of mankind. A lot of investigations have been carried out to bring the convenience of these devices to the user. Among most of the electronic devices, there is one similar common design which is printed circuit boards (PCB). PCB exists in most of the electronic devices as the platform to hold the components and integrated circuit (IC) in places while connecting the components with transmission lines.

Therefore, the reliability of the PCB with components is always an interest for researchers. In the past few decades, many researchers had studied the characteristics of the PCB so that proper design and handling process could be done to ensure the quality and durability of the electronic assembly on PCB such as Arruda and Freitas (2007) who studied the effect of surrounding air on drop test of flexible PCB (FPCB). When under operating condition, one of the major issues is the overheating of IC and electronic components. Some of the devices use active cooling method which is using fan to create air flow for cooling the IC and components. It is one of the cheapest ways to cool down the device. However, when FPCB is exposed to flow environment, FPCB would encounter unwanted deflection and stress. Further elaboration on PCB and FPCB will be presented in the following subsections.

1.2 Printed Circuit Board

1.2.1 Rigid PCB

PCB was invented by Albert Hanson in 1903 (Petherbridge et al., 2005). Most of the electronic devices contain PCB. The core material of PCB is FR-4 which is a composite material consisting of epoxy and woven glass. In the past two decades, rigid PCB (RPCB) was widely used as the substrate in modern electronic devices. Therefore, various studies on the reliability of the RPCB with components were conducted. Most of the reliability issues on RPCB include bending stress, mechanical shock/drop impact, joints connection and one of the major issues is the thermal stress. Figure 1.1 shows the open circuit faults on RPCB in mobile phones as marked in red arrows, which is also another issue encountered in RPCB (Ji et al., 2010). Components and IC always produce heat when in operation where different coefficient of thermal expansion (CTE) values of various materials would cause those materials expand in different rate which lead to high stress between materials. The thermal stress is harmful to the RPCB especially interconnection joints. Hence a lot of investigations have been carried out on heat transfer for electronic cooling. The fundamental of the numerical simulation and experimental setup for heat transfer on PCB are built up from those investigations.

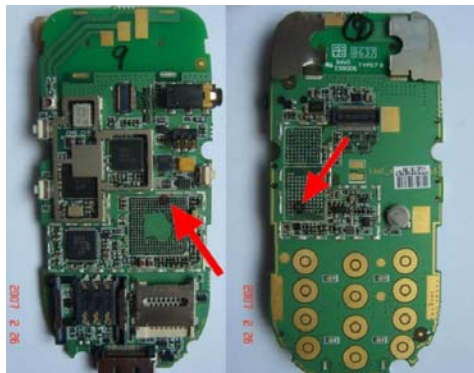

Figure 1.1: Rigid PCB in mobile phone (Ji et al., 2010).

1.2.2 Flexible PCB

With the rapid growth of electronic and microelectronics industries where mechanical flexibility is one of the crucial elements, FPCB has gained increasing popularity. FPCB has been used as an alternative to RPCB in several fields due to its lighter weight, lower cost, more robust, better twistability and flexibility (Xiao et al., 2008). The core material of FPCB usually made of either polyimide, polyethylene, polyester or naphthalate (Leong et al., 2012a). Polyimide provides several advantages compared to other materials such as low cost, wide available thicknesses range and good mechanical stress tolerance (Rujun et al., 2016). As shown in Figure 1.2, typical FPCB consist of electrically conductive layer (copper) and electrically resistive layer (polyimide). Researchers have used FPCB in several applications such as fabricated and mounted flow sensor on the FPCB for heat and flow detection, flexible wet sensor sheet to detect urination in diapers and applied FPCB in motor, coil and electrodynamics bearings (Dehez et al., 2014; Guoping et al., 2015; Petropoulos et al., 2012; Que Rui Yi and Zhu Rong, 2015; Takamiya et al., 2014; Wang et al., 2014). The reliability issues on FPCB (i.e. bending stress, mechanical shock/drop impact, joints connection and thermal stress) are similar to RPCB, just that FPCB has better flexibility to absorb more impact. However, the soft nature of FPCB unavoidably encounters more deflection and stress as compared to RPCB in the flow and operating environment.

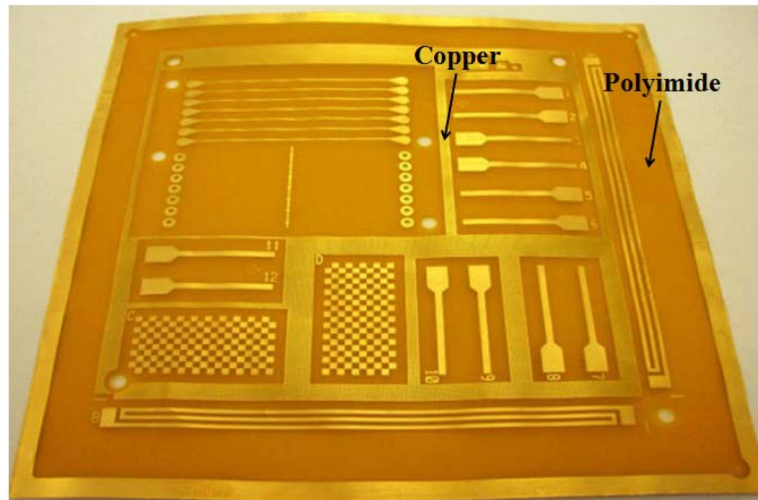

Figure 1.2: Typical flexible PCB (Rizvi et al., 2010).

1.3 Problem Statements

The rigid feature in RPCB becomes constraint in some modern electronic or microelectronic devices. Therefore, FPCB becomes popular and as an alternative to RPCB. Previous researches focused more on the thermal stress and cooling effect on the RPCB while deflection and stress induced by flow was often ignored as it is insignificant for RPCB (Arruda and Freitas, 2007). However, FPCB inevitably confronts more deflection and stress under flow environment compared to RPCB. Former studies only investigate FPCB with simple Perspex blocks to represent the components in numerical simulation and experiment. Besides, previous studies were limited to the flow effect on FPCB (Leong and Abdullah, 2012; Leong et al., 2012a). In other words, the FPCBs in those studies were in idle state. Thus, the study of FPCB behaviour in operating condition is necessary so that the deflection, stress and thermal effect on FPCB could be controlled and reduced. Hence, thermal factor should be included and coupled simultaneously with flow effects.